Air as dilute water: Passive air sampling reveals water-to-air transfer of environmental DNA

Yin Cheong Aden Ip[1]*, Gledis Guri[1]*, Elizabeth Andruszkiewicz Allan[1], Ryan P. Kelly[1]

School of Marine and Environmental Affairs, University of Washington, Seattle,

1   Washington, USA

*   shared first authorship

corresponding author **adenip@uw.edu**

Abstract

Water and air are generally treated as separate reservoirs of environmental DNA (eDNA) derived from the species resident in those respective environmental compartments. However, it is likely that eDNA routinely crosses the air-water boundary in both directions as a result of deposition, evaporation, or other processes. Here, we systematically tested methods of sampling eDNA at the air-water interface, showing for the first time that aquatic life can be consistently detected under standardized field conditions from passive air samples. We deployed four simple air samplers — three different kinds of filters and one open tray of deionized water — alongside paired water samples and visual counts over a six-week peak run of Coho salmon (*Oncorhynchus kisutch*) at a local spawning stream. We then quantified eDNA concentrations in both air and water (air: copies/cm^2/day; water: copies/L) using quantitative PCR, to estimate (1) the concentration of target eDNA in air vs. water, and (2) the capture performance of each filter

type. Passive air collectors captured quantitative airborne eDNA signals that covaried with

salmon counts, despite air eDNA concentrations being approximately 25,000 times more dilute

than water, although eDNA recovery varied with sampler design and orientation. We show the

air-water interface can be a quantifiable source of aquatic genetic information in this system

using simple, passive samplers that do not require electricity, making them appealing for

biomonitoring in remote or resource-limited settings. This work points the way to using airborne

eDNA as a promising pathway for biological information critical to conservation, resource

management, and public-health protection.

Keywords: environmental DNA, Air eDNA, Passive Air Filtration, Aquatic
Biomonitoring, Aerosolization, Evaporation, Non-invasive Sampling, Quantitative eDNA
Analysis, Salmon, Environmental Genomics

1. Introduction

Monitoring aquatic life is fundamental to understanding ecosystem health, guiding
conservation efforts, and managing valuable natural resources[1,2]. Over the past decade,
environmental DNA (eDNA) has revolutionized biodiversity assessment by detecting extra-
organismal DNA—genetic material shed by organisms into their surroundings. With appropriate
calibration or models, eDNA can track organismal presence or abundance[7]. Water-based eDNA
surveys have proven particularly effective for monitoring endangered species[3], early detection of
invasive species incursions[4], characterizing community composition[5], and even providing
quantitative assessments for complementing traditional surveys[6–8].

Meanwhile, airborne eDNA research has emerged as a promising frontier, though to date
it has focused almost exclusively on terrestrial organisms. Both active and passive air filtration

40   methods have been shown to recover DNA from mammals, birds, insects, and plants under field

41   and enclosed conditions[9–15]. Intriguingly, these same air-sampling techniques sometimes detect

42   aquatic taxa. For example, Tournayre et al. [16] reported the occurrence of aquatic species in air

43   eDNA samples, but the authors emphasized that the underlying mechanisms responsible for

44   these detections remain unclear, suggesting multiple, non-exclusive scenarios including prey

45   DNA and soil re-suspension. Crossover signals between air and water have not yet been the

46   focus of a study and are often treated as suspected contamination or attributed to feed or

47   piscivores fecal bioaerosols[15,17–19], rather than as a genuine ecological signal[16]. As a practical

48   matter, aquatic species signals detected in airborne eDNA surveys are often discarded[17-21], yet

49   these overlooked detections can hint to an untapped source of real genetic material hence

50   ecological inference.

51   Environmental systems are inherently interconnected[20], and basic physics implies that

52   aquatic DNA should appear in air[21,22]. Natural physical processes at the air-water interface —

53   such as evaporation, bubble-burst aerosolization from riffles, and biological processes such as

54   splashes, leaping fish, and churning substrates creating aerosols —all provide plausible

55   mechanisms for transferring eDNA from the water into the air[23–26]. Despite parallel advances in

56   aquatic and airborne eDNA research[18,19,27,28], the question of whether aquatic genetic material

57   naturally and routinely moves across media into the air has remained untested.

58   Existing work has characterized the shedding, transport, and decay of environmental

59   DNA[49,51,53,54], indicating that such processes can shape its concentration in the medium. Yet rates

60   are strongly context dependent, varying with hydrodynamic conditions, turbulence, temperature,

61   UV exposure, substrates, and species behavior, hence, generalized predictions are

62   challenging[48,51,54]. Rather than estimating each component in isolation, other studies have treated

63   their combined effect with a single integrated parameter that enables linking observed fish

64   abundance to measured eDNA, providing a practical, system-specific calibration while

65   acknowledging process complexity[7]. Such integrated approaches have been applied to aquatic

66   eDNA (from trawls and water samples[7,37]) and to active airborne eDNA samplers, but never to

67   passive air samplers, and crucially, never to paired air-water measurements that would allow

68   quantification of cross-medium transfer.

69   We conducted the first targeted investigation of cross-medium water-to-air eDNA

70   transfer, specifically examining whether genetic material from aquatic organisms can be detected

71   in air samples collected above the water surface. Leveraging the behavior of Coho salmon

72   (*Oncorhynchus kisutch*) during their spawning season[24], we collected and measured eDNA

73   concentrations in paired water and passive air samples over a six-week peak migration period,

74   with visual fish counts from the staff of a fish hatchery. To evaluate the mechanisms of airborne

75   DNA capture and settlement, we deployed four passive air collection methods: vertically

76   oriented gelatin air filters (commonly used in low-flow air filtration systems),

77   polytetrafluoroethylene filters (PTFE; standard in high-flow air applications), and mixed

78   cellulose ester filters (MCE; traditionally employed for water filtration), as well as an open,

79   horizontal tray of deionized water exposed to ambient conditions[18]. These were chosen for their

80   distinct physical properties, contrasting orientations, and different particle capture efficiencies

81   targeting different aerosol types. By comparing detection sensitivity, temporal patterns, and

82   quantitative performance of these four collectors against water eDNA concentrations and visual

83   counts, we tested if airborne eDNA can consistently track real-world aquatic population

84   dynamics and which filter type would track biological signal most appropriately.

85   Our overarching goal was to test whether airborne eDNA can quantitatively track aquatic

86   organisms under natural field conditions. Specifically, we hypothesized that (1) DNA from

87   spawning salmon would be detectable in passive air samples collected above the water surface,

88   (2) airborne eDNA concentrations would covary with co-located water eDNA and with visual

89   fish counts, and (3) passive sampler types would differ in the fraction of signal captured because

90   of particle-size and deposition dynamics. This study provides a systematic, field-based

91   investigation of water-to-air eDNA transfer in a natural stream, complementing prior airborne

92   eDNA work that has focused on terrestrial taxa, and offers a transferable framework for other

93   regions and study systems, while recognizing that replication across seasons, sites, and taxa will

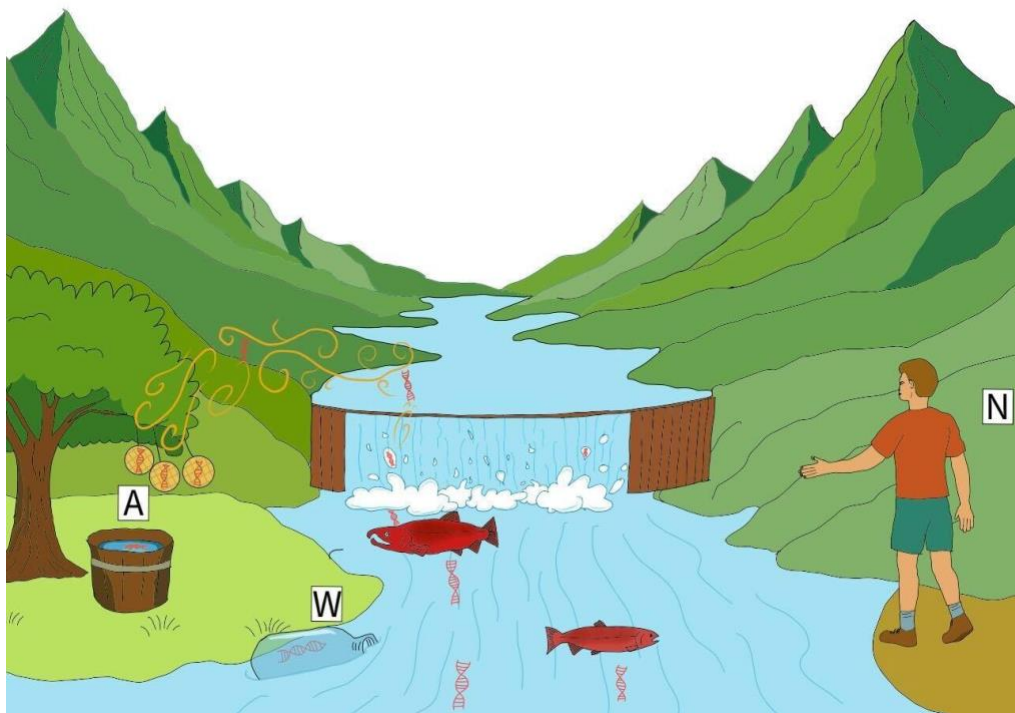94   be needed to assess broad applicability.

95

96   *Figure 1: Conceptual illustration of cross-medium eDNA sampling above a salmon-spawning stream.*
97   *Natural processes, including evaporation, bubble-burst aerosolization at riffles and splashes, and the*
98   *vigorous movement of spawning Coho salmon, launch trace amounts of DNA from the river surface into*
99   *the atmosphere. Passive airborne samplers, shown here as three vertically hung filters and an open tray*

100 *of deionized water (A), intercept settling airborne eDNA, while paired water-grab sampling (W) and*
101 *visual counts by hatchery staff (N) provide concurrent reference measurements.*

2. Methods

2.1 Field Sampling

104   We conducted this study near Seattle, Washington USA, in Issaquah Creek, a salmon

105 spawning stream, outside of the Issaquah Salmon Hatchery (47.529501° N, 122.039133° W)

106 from 17 October 2024 to 21 November 2024, with six sampling events. Issaquah Creek is a

107 tributary of Lake Sammamish that drains approximately 175 km² of mixed forested and urban

108 watershed in the Cascade foothills, with discharge of 30-50 cfs (0.8-1.4 m³/s) during the study

109 period. The creek supports natural runs of Chinook and Coho salmon, with the Issaquah Salmon

110 Hatchery operating at this location since 1936. The study site was in a riparian corridor

111 approximately 3 km upstream from the creek's mouth at Lake Sammamish, where the watershed

112 transitions from forested headwaters to developed lowland areas.

113   We sampled at six time points that spanned the entire Coho salmon (*Oncorhynchus*

114 *kisutch*) run, from the first arrivals in early fall of August through peak abundance around 17

115 October 2024 and into the tail end of the migration in November. This schedule ensured that our

116 eDNA sampling captured both the lowest and highest levels of fish activity. Within the same

117 sampling period, visual fish counts were performed by the hatchery staff, and salmon

118 escapement data were obtained from the Washington Department of Fish and Wildlife

119 escapement reports (https://wdfw.wa.gov/fishing/management/hatcheries/escapement#2024-

120 weekly). The hatchery operates a fish ladder with gates that are opened periodically by staff, who

121 conduct visual counts of accumulated fish before allowing passage. This controlled system

122 ensures that all Coho salmon in the study area are counted at this single point before entering the

123 hatchery, creating a direct correspondence between visual counts and the fish population

124 generating eDNA signals in our sampling area. Weather conditions varied throughout the

125 sampling period; environmental metadata for each sampling date—precipitation and mean daily

126 river discharge—are provided in (SI Appendix, Table S2).

127 **2.2 Airborne eDNA sampling**

128 Sampling for eDNA was conducted in 24-hour blocks with deployment and recovery

129 around 9 a.m. (river water was collected only on the first day of each of the six sampling

130 timepoints). Four passive collection methods were evaluated: three filter types—gelatin

131 (Sartorius, 47 mm diameter), PTFE (Whatman, 47 mm diameter), and MCE (Sterlitech, 5.0 μm

132 pore size, 45mm diameter)—and an open container of deionized water. The rationale for

133 selecting these materials is as follows: gelatin filters are effective at capturing airborne particles

134 and are particularly suited for applications where maintaining viability (e.g., for subsequent

135 bacterial culturing[29]) is desired; PTFE filters are noted for their high durability and are widely

136 used in active air sampling experiments[30]; whereas MCE filters, typically employed for water

137 filtration, were included to assess their performance in an airborne context[6]. All three passive

138 filters were deployed via custom 3D-printed "honeycomb" puck filter holders, based on open-

139 source Thingverse designs (IDs 4306478 and 979318; Zachary Gold, pers. comms.), and were

140 suspended from a hatchery railing approximately 3 m above the river water level (Figure 1), with

141 their collection surfaces oriented vertically. This configuration minimized splash contamination

142 and captures airborne DNA particles driven by gravitational settling. The positioning relative to

143 flowing water demonstrated how these passive collectors operate at a vantage point above the

144 stream, facilitating non-invasive DNA capture in real-world field conditions. Two biological

145 replicates were deployed for both gelatin and PTFE, while only one replicate was used for MCE.

146 After the overnight deployment, filters were carefully recovered using sterile, disposable forceps

147 and immediately immersed in 1.5 mL of DNA/RNA Shield.

148   The fourth passive collection method was an open container (25 cm width, 30 cm length,

149 10 cm depth) filled with 2 L of deionized water[18] also positioned about 3 m above the river and

150 about 30 cm above the suspended passive filters. The open container was also deployed for about

151 24 hours at the same times as the passive filters. The container had an open surface (i.e., oriented

152 horizontally) to capture airborne particles settling by gravity. The surface area of the container

153 was approximately 750 cm^2, in contrast to the roughly 16 cm^2 surface area offered by the 47-

154 mm circular filter disks. Only one replicate was used for the open water container method. Note

155 that although 2 L of deionized water was placed in the container, heavy rainfall during overnight

156 deployments sometimes increased the water level. Any debris (e.g., bugs, leaves) was removed

157 from the container before on-site filtration using the same system as for river water samples (see

158 below for details).

159 **2.3 Water eDNA sampling**

160   At each of six sampling events, we collected one 3 L surface-water grab (3 × 1 L

161 biological replicates) at a fixed site immediately downstream of the fish-ladder gate, adjacent to

162 the Coho salmon aggregation area and concurrent with air deployments. Water was collected in

163 sterile bottles, directly adjacent to the aggregation area. The ladder is operated continuously by

164 hatchery staff throughout the salmon run, ensuring fish passage and visual counts. A total of 3 L

165 of water was filtered on site using a Smith-Root Citizen Science Sampler equipped with 5.0 μm

166 mixed cellulose ester (MCE) filters[6]. Three 1 L replicates were processed and immediately

167 preserved in 1.5 mL of DNA/RNA Shield (Zymo Research) using clean disposable plastic

168 forceps. Field-negative filtration blanks (1 L of Milli-Q water each) were also processed using

169 the same system. All equipment was decontaminated with 10% bleach, thoroughly rinsed with

170 deionized water, and handled with gloves to minimize contamination. All filters (passive air,

171 passive open container, water) were stored at –20°C until processing, typically within one week.

172 The ladder site concentrates upstream migrating Coho salmon and is the control volume where

173 fish are enumerated; sampling water at this location keeps measurements co-located with the

174 airborne collectors and the visual count. One 3 L sample per event provided six time-matched

175 water–air pairs for estimating the water-to-air transfer parameter η in the joint model (see section

176 2.5). In this design, water serves as a calibrated comparator for airborne eDNA[36,37]. This single

177 water sample per event was the paired water measurement used in the joint model.

178 **2.4 Wet-Laboratory Procedures**

179 　DNA extraction from both river water samples and airborne filter samples was performed

180 using the Qiagen Blood and Tissue Kit according to the manufacturer's protocols. During

181 extraction, it was noted that the gelatin filters dissolved completely in the DNA/RNA Shield.

182 Samples were vortexed for 1 minute, and 500 μL of the shield was used for DNA extraction.

183 　qPCR assays targeted a 114-bp fragment of the cytochrome b gene of Coho salmon,

184 using the forward and reverse primers derived from Duda et al. 2021[34]— COCytb_980-1093

185 Forward: CCTTGGTGGCGGATATACTTATCTTA and COCytb_980-1093 Reverse:

186 GAACTAGGAAGATGGCGAAGTAGATC. Although Duda et al. validated a TaqMan (probe-

187 based) assay, we used SYBR Green chemistry with the SYBR Select Master Mix (Fisher

188 Scientific) and verified specificity by melt-curve analysis; on an Applied Biosystems

189 QuantStudio 5 real-time PCR system with a 384-well block. Each 10 μL reaction consisted of 5

190   μL of SYBR Select Master Mix, 0.4μL of 10 mM forward primer, 0.4 μL of 10 mM reverse

191   primer, 2.2 μL of molecular grade water, and 2 μL of DNA template. Melt curve analysis was

192   performed to confirm the amplification of the target fragment, with an accepted melting

193   temperature of $81°C \pm 1°C$. All standards and positives showed a single melt peak at 81 $°C \pm 1$

194     $°C$, and no-template and field-negative controls showed no amplification.

195   Standard curves were constructed using a Coho salmon tissue DNA extract quantified

196   with a Qubit fluorometer SI Appendix, Fig. S6. The stock solution was diluted to 1.0 ng/μL and

197   designated as 10^6 copies/μL. Serial dilutions were then prepared, with 10^5, 10^4, and 10^3

198   copies/μL run in triplicate, 10^2 copies/μL in quadruplicate, and 10^1/μL copies in triplicate.

199   Assay performance was summarized by the qPCR standard curve and a detection-probability

200   curve derived from replicate standards (SI Appendix, Fig. S6), and this observation-level

201   uncertainty was propagated in the hierarchical model; accordingly, we reported these

202   performance curves rather than fixed LOD/LOQ thresholds.

203 2.5 Joint statistical model

204 2.5.1 Visual observation model

205   In summary, we synthesized three methods of observations (visual counting of fish, water eDNA

206   measurements, and air eDNA measurements) that derived from a single unknown true fish

207   accumulation rate (denoted here as X). This joint approach allowed us to estimate the

208   aerosolization factor (η; the magnitude of water eDNA transferred to air), the effectiveness and

209   reliability of different passive air filtering techniques (τ), and the replicability of various filters

210   (ρ) throughout the 6-week peak Coho salmon spawning period. Accordingly, the water

211   measurement at the fish ladder counting site was used as a time-matched index of local fish

212   density that drove the air compartment in the joint model. At each sampling event, we obtained

213   one water measurement at the ladder site and contemporaneous air measurements from the

214   passive air collectors (by filter type with biological replicates). The aerosolization parameters

215   were estimated from the six paired water–air observations across the study period.

216   We modeled the upstream migration of Coho salmon (*Oncorhynchus kisutch*) as arising

217   from the inferred unknown true density of fish, X. As individuals moved upriver, fish

218   accumulated in a holding area immediately downstream of the hatchery river dam (our water and

219   air sampling location). At discrete times t (six weekly sampling dates between 17 October and

220   21 November 2024), the hatchery staff opened the ladder gate to allow passage into holding

221   tanks. Between successive gate-opening events (Δt), additional Coho salmon arrive and join the

222   backlog in the holding area, increasing the number of individuals awaiting passage. We denoted

223   the true daily accumulation rate X_t (also fish density at the river dam) in units of fish/day at time

224   t, and we denoted the counting effort as E (measured as the elapsed number of days between

225   consecutive gate openings; $E_t = \Delta t$; hence $E_{t=1} = 0$). Here, E_t (days) represented the count

226   effort, converting the daily accumulation rate X_t (fish/day) into the expected accumulated count

227    $\lambda_t = X_t \cdot E_t$ (fish) in Eq. (1). Counts were full enumerations at the ladder immediately before

228   each opening and hence, person-hours are not modeled separately. Prior to each gate opening (at

229   time t), the hatchery staff conducted a visual count N_t of accumulated fish. Assuming X_t

230   remained relatively constant between successive gate-opening events (Δt), we modeled the

231   observed fish counts as a Negative Binomial process:

232    $$\lambda_t = X_t \cdot E_t \tag{1}$$

233    $$N_t \sim Negative\ Binomial(\lambda_t, \phi) \tag{2}$$

234   where, N was the visually observed number of fish at time t, λ_t was the expected number

235   of fish accumulated over the E_t-day interval with a fixed overdispersion parameter shared across

236   time points ($\phi = 20$; hence variance $\lambda + \frac{\lambda}{\phi}$)[7,32]. Given the small number of time points (n = 6),

237   the overdispersion parameter φ was fixed to a literature-supported value rather than estimated.

2.5.2 Molecular process model

239   We denoted W as the unobserved eDNA concentration (copies/L) in the single water

240   sample collected at each time point t and ω as the "integrated eDNA factor" – the conversion

241   factor between fish accumulation (X) and eDNA concentration (W; see[7] for further interpretation

242   of ω). Here, ω was treated as a population-scale factor that aggregated per-fish eDNA emission

243   (i.e., the average shedding rate per individual), together with decay, transport, and dilution at the

244   site; we assumed it was approximately constant over the 24-h sampling window. Individual-to-

245   individual variation was not modeled explicitly and contributed to residual variance. We

246   expressed the relation between the fish density and water eDNA concentration as:

247
$$W_t = X_t \cdot \omega \tag{3}$$

248   We denoted A as the unobserved eDNA concentration (copies/cm^2/day in the air at time t

249   which was filtered using passive collection method j. We indexed air collection methods as j $\in$

250    $\{1…4\}$index air-collection methods: 1= PTFE, 2= gelatin, 3= MCE (air-suspended), 4= DI-water

251   tray. We modeled the air eDNA concentration as a log-linear function of the water eDNA with

252   intercept η, slope = 1, and error term ε (unexplained variability; time and filter specific):

253
$$ln\left(A_{tj}\right) = \eta_j + ln(W_t) + \varepsilon_{tj} \tag{4}$$

254   Here, the intercept η was interpreted as the water-to-air transferability (or dilution) factor

255   and ε as the error term parameter (similar to the sum of squares error) from a linear regression

256   where $\varepsilon_{tj} \sim N(0, \tau_j)$.

257   For the two filter types with biological replicates ($j \in \{1,2\}$; PTFE and gelatin) ; we

258   sampled two biological replicates and we used the mean of those biological replicates to

259   determine the average concentration in the air A at time t as following:

260
$$ln\left(A_{tjb}\right) = ln\left(A_{tj}\right) + \delta_{tjb} \qquad for\ j \in P, G \tag{5}$$

261   where δ_b indicated the deviation of individual biological replicate from the average

262   concentration (A_{tj}), following a normal distribution with mean 0, $\delta_{tjb} \sim N(0, \rho_j)$, with ρ_j

263   indicating the magnitude of the replicates deviation from the mean sample. Because we had only

264   two replicates at each sampled time, we imposed a sum to zero constraint on the replicates (b)

265   collected from a single sampling time ($\sum_b \delta_{tj} = 0$).

266   To estimate the levels of eDNA concentration in water (W) and air (A), we utilized the

267   qPCR observation models (as described in[33,34] with slight modifications). The model

268   compartment utilized the standard curve samples to estimate the intercept ($\phi, \beta0, \gamma0$) and slope

269   ($\beta1, \gamma1$) parameters between the known concentration (K) and the observed data (Z and Y) from

270   qPCR machine as follows:

271
$$
\begin{aligned}
Z_{kr} &\sim Bernoulli(\psi_k) & (6)\\
\psi_k &= 1 - exp(-K_k \cdot \theta) & (7)\\
Y_{kr} &\sim Normal(\mu_k, \sigma_k) \quad if Z_{kr} = 1 & (8)\\
\mu_k &= \beta_0 + \beta_{1p} \cdot ln(K_k) & (9)\\
\sigma_k &= exp(\gamma_0 + \gamma_1 \cdot ln(K_k)) & (10)
\end{aligned}
$$

272   where we denoted Z as the binary outcome of target amplification for sample (k) and

273   technical replicate (r) being present (1) or absent (0) following a Bernoulli distribution given the

274   probability of detection ψ for each sample (k). We denoted the parameter ϕ as the intercept of

275   the function between probability of detection ψ and the known DNA concentration $(K$;

276   copies/μL reaction) as the predictor variable. Additionally, for equations 8-10, Y was the

277   observed cycle threshold (Ct) for sample (k) and technical replicate (r) which followed a normal

278   distribution with mean μ (mean Ct) and standard deviation σ for each sample (k). We modeled μ

279   as a linear function of known eDNA concentration (K) with intercept $\beta0$ and plate specific (p)

280   slope $\beta1$ and the standard deviation σ of the observed Y as an exponential function of known

281   eDNA concentration with intercept $\gamma0$ and slope $\gamma1$.

282   Subsequently, we built the same model compartment for estimating eDNA concentration

283   in water and air by substituting U_t and Q_{tj} (and Q_{tjb} for $j \in \{1,2\}$) respectively, with K_k through

284   equation 6-10 (see SI Appendix, Fig. S1), where U and Q are concentration normalized per

285   reaction volume ($V = 10\ \mu$L for all reactions including water and air samples), water volume

286   filtered in the field (F = 1 L for all water samples), surface area ($S = 16\ \text{cm}^2$ for gelatin, PTFE,

287   and MCE, and 750 cm^2 for the open containers of deionized water; for air samples only) and for

288   passive deployment time (P = 1 day across all samples at all time t; for air samples only) of W

289   and A respectively as follows:

290    $$U_t = W_t \cdot \text{F} / \text{V} \tag{11}$$

291    $$Q_{tjb} = A_{tjb} \cdot S_{tj} / \text{V} \cdot \text{P} \tag{12}$$

292   The intercept and slope parameters (from equation 7, 9, and 10) between qPCR

293   observations and eDNA concentration of water, air and the standard samples were shared

294   between model compartments.

295   **2.6 Model conditions**

296   The joint model (SI Appendix, Fig. S1) was implemented using the Stan language as

297   implemented in R (package: Rstan) running four independent MCMC chains using 5000 warm-

298   up and 5000 sampling iterations (for parameters and their prior distributions see SI Appendix,

299   Table S1). The posterior predictions were diagnosed using statistics (Gelman and Rubin 1992)

300   and considered convergence for values less than 1.05 and effective sample size (ESS) greater

301   than 1000 for all parameters. Additionally, the posterior predictive checks were used with results

302   presented in the SI Appendix, Fig. S5. Observations from different gate-opening intervals were

303   assumed independent; with n = 6, we did not fit an explicit temporal correlation structure.

3. Results

305   Airborne eDNA was detected across all passive methods and covaried with Coho salmon

306   abundance in the river during the upstream migration period. Detection efficiency and signal

307   strength varied considerably among the different passive airborne eDNA capture methods. We

308   then estimated the water-to-air dilution factor and compared temporal congruence among

309   collectors to identify which designs best tracked the biological signal.

3.1 Fish accumulation based on visual counts and eDNA in river water

311   Coho salmon migration occurs not as a single continuous event, but rather as a series of

312   distinct burst peaks from mid-October through late November, where the peaks are highly likely

313   to be connected with environmental factors such as water temperature and discharge. The

314   average daily accumulation rate (X; black line in Figure 2) was estimated at 160.4 fish/day with

315   peaks exceeding up to 286 fish/day and low activity of ca. 78 fish/day (Figure 2).

316   Because both observation methods (river water eDNA and visual observation) are jointly

317   used to estimate the daily accumulation rate (X), their concordance was best evaluated through

318   the parameter ω. A converged and narrowly distributed ω parameter indicates strong agreement

319   between the two methods and simultaneously a reliable conversion parameter from fish/day to

320   eDNA copies/L. In this case, $\omega = 9.578$ (95% quantile range of 9.352 to 9.804; (SI Appendix,

321   Fig. S4)), suggesting consistent concordance between observed fish counts and eDNA

322   concentrations hence, biologically, this implies that an accumulation rate of 1 fish/day

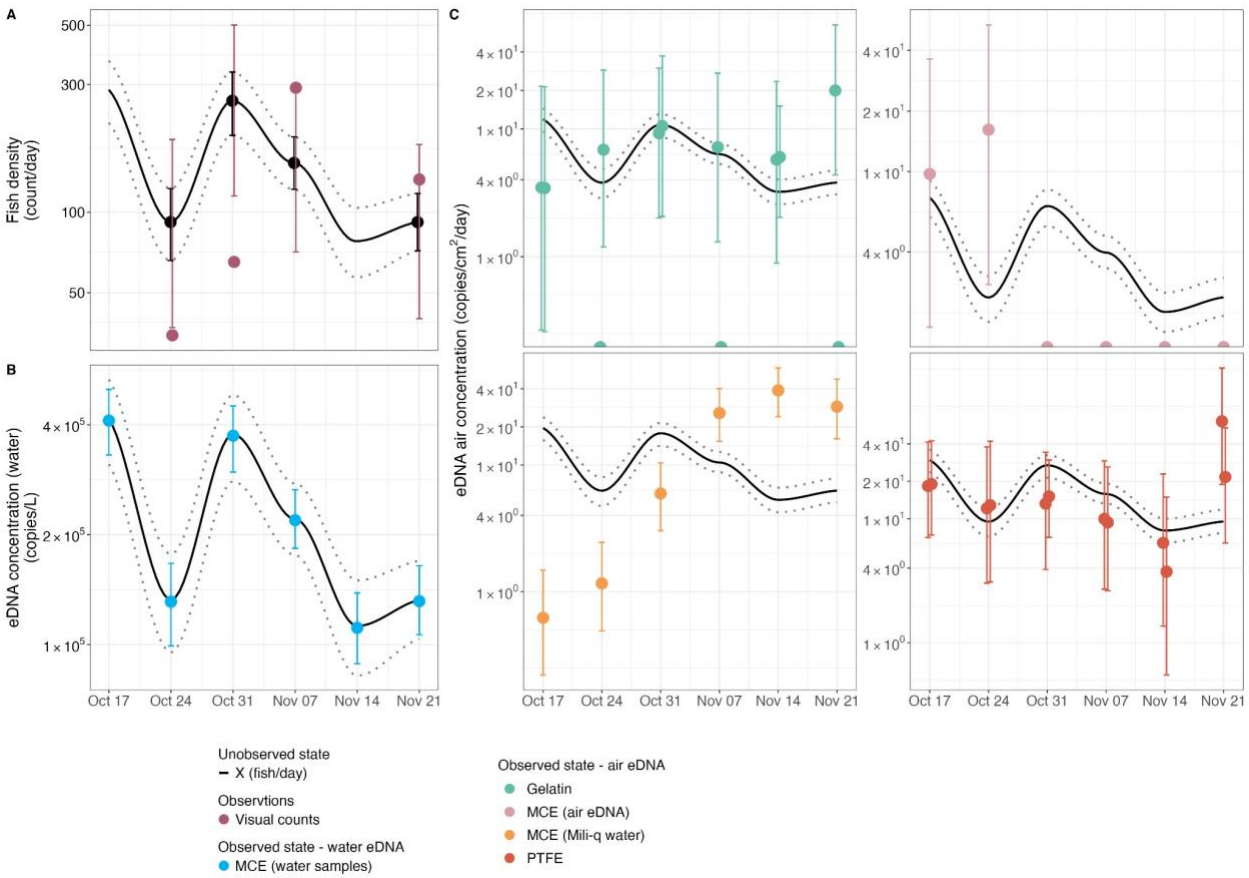323   corresponds to approximately 15000 ($\pm$ 3000) copies/L.

324

Figure 2: The temporal dynamics of estimated fish density in units of fish/day (X; black smoothed line with 95 confidence intervals - dotted lines - and their posterior estimates with 95% confidence intervals bars) from 17 October to 21 November compared to the posterior distributions (and 95% confidence intervals indicated by vertical bars) of eDNA concentrations (copies/L) in water (B), and eDNA concentrations (copies/cm^2/day) in air using various filter types (C). In panel A we also show the observed visual counts (dark rose dots) normalised per counting effort (E) with the 95% posterior probabilities (dark rose bars) derived from the Negative binomial distribution with mean X (fish density) and the fixed overdispersion parameter ($\Phi=20$). The jitter in x-axis for panel A and for Gelatin and PTFE plots in panel C are for visualization purposes only, i.e., no difference in collection dates.

3.2 Air eDNA signals

Airborne eDNA originating from Coho salmon was successfully detected across all passive air collection methods deployed (gelatin, PTFE, MCE filters suspended in air, and open containers of deionized water - MCE DI water). Across airborne sampling approaches, airborne eDNA concentrations were approximately 25,000× lower than co-located water concentrations

341   (ranging ~15,000–50,000× depending on sampler type; Table 1; SI Appendix, Fig. S2A). These

342   values are summarized by an integrated dilution parameter (η) defined in Methods (Table 1; SI

343   Appendix, Fig. S2A). Despite the general consistency in estimating the water-to-air dilution

344   coefficient, method-specific variations in collection efficiency were observed (Table 1; SI

345   Appendix, Fig. S2A). PTFE filters exhibited higher capture efficiencies, collecting 2 times more

346   eDNA than the mean across all air sampling methods (Table 1). Deionized water tray (MCE DI

347   water) demonstrated the second highest efficiency (1.3 times the average; Table 1), while gelatin

348   filters and air-suspended MCE filters showed comparatively lower capture efficacy (0.8 and 0.5

349   times the average, respectively; Table 1).

350   In terms of alignment with the biological activity, PTFE and gelatin filters showed the

351   strongest covariation with the daily fish accumulation patterns, exhibiting the lowest residual

352   error magnitude (expressed as the standard deviation of ε) with $\tau = 0.473$ and 0.570, respectively

353   (Table 1; SI Appendix, Fig. S2B). Conversely, MCE DI water, despite having the largest surface

354   area, showed less agreement with the fish migration dynamics ($\tau = 1.780$; Table 1; SI Appendix,

355   Fig. S2B). The MCE air suspended filters performed least effectively in tracking temporal

356   migration patterns, failing to amplify Coho salmon DNA beyond the first two weeks of the

357   sampling campaign Figure 2C.

358   Subsequently, biological replicates for gelatin and PTFE filters revealed additional

359   insights regarding methodological robustness and reproducibility. PTFE filters produced the

360   most consistent quantifications, with lower variance (expressed as the standard deviation of δ)

361   between replicates ($\rho = 0.154$; Table 1; SI Appendix, Fig. S2C), whereas gelatin filters showed a

362   higher degree of variability ($\rho = 0.386$; Table 1; SI Appendix, Fig. S2C), indicating reduced

363   reproducibility of quantitative outcomes.

364   In sum, these performance differences across sampling methods likely reflect inherent

365   physical and operational characteristics of each filter type and collection method, which in turn

366   influence their ability to capture either discrete or cumulative biological signals from the source

367   species.

368   *Table 1. Estimated posterior means of dilution parameter (η), standard deviation of the residuals*

369   *(τ), biological replicability (ρ), and capturing efficiency ($e^{(\eta - \underline{\eta})}$)*

Filter type	Dilution (in log_e) (η)	Standard deviation (τ)	Biological rep. error magnitude (ρ)	Capturing efficiency $e^{(\eta - \overline{\eta})}$
Gelatin	-10.45	0.473	0.386	0.785
PTFE	-9.53	0.570	0.154	1.979
MCE Air	-10.91	0.949	-	0.496
MCE DI water	-9.95	1.780	-	1.295

370

3.3 Model diagnostics

372   Convergence and reliability of the Bayesian model were assessed through comprehensive

373   diagnostics. All parameters (SI Appendix, Table S1) exhibited reliable Gelman-Rubin

374   convergence statistics ($\hat{R} < 1.01$) and effective sample sizes (ESS) exceeding 1000 per

375   parameter, indicating successful convergence and efficient mixing of the four independent chains

376   (SI Appendix, Fig. S3*A*). No divergent transitions were detected during sampling, and the

377   maximum tree depth was not exceeded, indicating no issues with divergence or exploration

378   limits (SI Appendix, Fig. S3*B*). The posterior likelihood demonstrated convergence before the

379   sampling phase began, with all chains exhibiting high mixing, confirming robust exploration of

380   the parameter space (SI Appendix, Fig. S3*B*).

381   Prior sensitivity analyses revealed that posterior estimates differed from priors,

382   demonstrating that the posteriors were appropriately updated based on the observed data rather

383   than being heavily influenced by prior assumptions (SI Appendix, Fig. S4). Additionally, the

384   posterior predictive checks (PPC) demonstrated that the model reliably reproduced the observed

385   data, supporting the validity of parameter estimates (SI Appendix, Fig. S5). Collectively, these

386   diagnostics confirm the reliability and validity of the Bayesian model used here.

387   ## 4. Discussion

388   **4.1 A new dimension of biodiversity monitoring**

389   Our study shows, for the first time, a field-based proof-of-concept that passive airborne

390   eDNA sampling can capture and track molecular signals from aquatic organisms. In this

391   system—Coho salmon in a hatchery-controlled river reach—fully passive airborne eDNA

392   sampling (no active airflow) recovered salmon genetic material and covaried with water eDNA

393   concentrations and visual counts of salmon across six weekly sampling events, providing proof-

394   of-concept in this context that the air and water assays reflected a common underlying

395   phenomenon. This suggests a new and complementary pathway for assessing aquatic

396   biodiversity – through the air, without ever touching the water. In salmon-spawning streams,

397   genetic material from the river is transported into the air likely by evaporation, bubble-burst

398   aerosolization at riffles and splashes, and the rigorous churning of spawning fish[35,36]. Collections

399   from multiple passive samplers, when compared with conventional water-based eDNA assays

400 and daily visual counts, were consistent with a quantitative relationship between airborne eDNA

401 concentration and salmon density.

402 Detections of aquatic taxa in airborne surveys are often dismissed as contamination[15,17–

403 19]. Our data suggest otherwise. In this system, the airborne salmon eDNA signal is consistent

404 with an ecological origin rather than laboratory or procedural artifact. Additionally, it is likely

405 that environmental conditions such as wind speed, relative humidity, and temperature can

406 determine the spatial and temporal distribution of the aerosolized aquatic eDNA[37,38]. For

407 example, high humidity and rainfall force rapid settling and very localized deposition while dry,

408 windy conditions might carry genetic plumes further distances downwind[39,40]. Although

409 quantifying these effects was beyond the scope of this study, they – together with hydrological

410 variables – should be considered when evaluating how passive samplers capture transient pulses

411 of biological activity.

412 **4.2 How sampler design may shape signal detection**

413 The interpretations below are mechanistic hypotheses consistent with our observed

414 patterns and prior studies; we did not test these mechanisms directly. In concordance with other

415 studies tracking real biological life[41], our passive filters deployed for 24-hours (vertically

416 oriented gelatin and PTFE) acted as higher-resolution "fish-activity" samplers. Such processes

417 can occur due to ambient air currents likely sweeping fine, splash-generated aerosols rich in

418 salmon DNA onto filter membranes, yielding traces of DNA that could rise and fall in sync with

419 live fish counts and water-eDNA levels[42]. In contrast, the large horizontal tray of deionized water

420 seemed to function more like a hydraulic-driven deposition trap. The tray saw a steady

421 accumulation of eDNA over the six weeks and thus could have been collecting more coarse

422   spray, foam, and decay-derived particulates from river turbulence and from decomposing

423   carcasses[36,43]. Because salmon carcasses often remain in shallow banks and backwaters as the

424   spawning season progresses, it is plausible that river turbulence and discharge could generate

425   larger droplets over decomposing tissue, potentially facilitating eDNA dispersal[35,44]. Although to

426   our knowledge there is no study that has investigated this process in particular, we hypothesize

427   that the coarse droplets settle rapidly and dominate deposition on horizontal collectors while the

428   fine fraction produced by active fish movement could be more volatile and under-represented.

429   This could explain the more discrete nature of signals recovered from gelatin and PTFE filters

430   vs. the more cumulative signal of the water tray (which may integrate both flow-driven and

431   decay-driven processes into a steadily rising accumulation curve). While carcass-derived

432   particulates are a plausible contributor to the cumulative signal observed in the horizontal tray,

433   we did not directly quantify the relative contributions of carcass material and live shedding.

434   Disentangling these sources will require targeted experiments that track release from live fish

435   and from decomposing tissue under controlled conditions.

436   The filter materials and operational context also shaped the air sampling performance.

437   PTFE filters, known for their durability, delivered the most consistent results of all the passive

438   filtration methods; gelatin filters yielded the highest sensitivity but showed greater variability;

439   mixed cellulose ester filters captured negligible airborne DNA; and the open tray, with roughly

440   50 times more surface area than the vertical filters, recovered the highest total DNA yield. These

441   samplers can respond differently to weather primarily due to their material composition. In the

442   physical form, through our visual observations when handling the air samples, PTFE filters are

443   generally unaffected by rain (always intact when retrieved), whereas gelatin filters typically

444   dissolve when wet. Housing is another tunable design variable[13]: enclosed or rain-shielded filter

445 holders may mitigate wetting and UV exposure while maintaining deposition. Our deployments

446 used open holders, which likely contributed to wetting of gelatin filters during rain events.

447 Additionally, the environmental variables might introduce some untestable trade-offs. For

448 example, heavy rain can dilute the accumulated eDNA but may also scour additional airborne or

449 splash-borne DNA into the water. Real-world debris, such as leaves, insects, sediment, can also

450 wash into the tray, increasing the risk of clogging or necessitating pre-filtration before DNA

451 extraction. Rain and wind can also deliver non-local DNA to open trays; while the time-matched

452 concordance with co-located water eDNA and visual counts (Figure 2) argues for a

453 predominantly local signal in this study, we cannot exclude external inputs. Although our sample

454 size is too small to quantify these opposing effects, future work should explicitly test how

455 precipitation intensity influences both concentration and total yield[12]. Targeted experiments with

456 co-measured meteorology and particle data will be required to test these mechanisms (see

457 Discussion 4.4).

458 **4.3 Airborne eDNA as a fraction of waterborne eDNA**

459 Across airborne sampling approaches, airborne eDNA concentrations were

460 approximately 25,000× lower than co-located water concentrations, with values by sampler

461 spanning roughly 15,000–50,000×, at levels approaching the lower limits of qPCR detection.

462 Informally, the air compartment can be viewed as a highly diluted reflection of the water signal

463 at this site, but we emphasize this is a descriptive metaphor, not a tested mechanism. Despite this

464 extreme dilution, our rigorous sampling, laboratory methods, and statistical models reliably

465 picked up those sparse molecules, obtaining consistent, quantitative signals across the entire

466 spawning season. To put this in perspective, dissolving a teaspoon of salt into a large aquarium

467 yields a similar dilution magnitude: only a tiny fraction of DNA shed into the water ever makes

it into the overlying air, yet those few copies suffice to track real-time salmon activity. In particular, vertically oriented filters intercepted transient eDNA peaks that rose and fell broadly in concert with visual counts, suggesting that even at extreme dilution, airborne eDNA can still capture fine scale changes in fish presence that reflect real-world population dynamics.

Longer passive-sampler deployments naturally accumulate more settled eDNA, but they also expose collected material to ultraviolet radiation, microbial degradation and fluctuating humidity, all of which erode DNA integrity over time[45]. Hinds et al.[46] showed that waterborne eDNA degrades with a half-life of hours to days under natural sunlight and microbial loads, suggesting that once deposited on the filter, airborne fragments may decay on comparable or even faster timescales. By contrast, Klepke et al.[18] found that passive air particle collections continued to accrue new species detections for up to 96 hours, without specifying when deposition begins to be outpaced by degradation. In practical terms, this could mean that in a longer deployment much of the DNA captured from early days may degrade before retrieval which potentially can skew the majority of signal by reflecting material deposited in the final timespan of sampling. Here, we show that selecting a 24-hour deployment is sufficient for capturing biological signals which might alleviate the potential limiting factor of post-deposition loss[12]. However, future work should explore these plausible interpretations by varying deployment lengths from a few hours to several days, and pairing them with controlled decay assays, for example by spiking synthetic DNA onto filters and tracking its persistence, to determine the point at which accumulation and degradation balance.

Our findings also agree with the recent work by Giolai et al.[41] who showed that passive air samplers outperform active pumps by sampling intermittent, DNA-rich plumes over long intervals and detecting greater species richness. In our streams, vertical filters captured transient

491 bursts of salmon eDNA in near real-time, while the open tray, and likely longer deployments,

492 would tend to smooth those peaks into an integrated signal. Contrastingly, active-pump systems

493 operating for only hours would average across plumes and risk overlooking fine-scale temporal

494 changes.

495 By systematically mapping this interplay between deposition and degradation, and by

496 benchmarking passive against active approaches, we can establish best-practice guidelines for

497 airborne eDNA sampling durations. This effort would mirror how water-based eDNA workflows

498 define optimal filtration volumes and storage times[27,47] and would enable robust, context-specific

499 deployments that maximize genuine signal recovery for real-time biodiversity monitoring.

500 Airborne eDNA decay dynamics remain largely unquantified. While aquatic decay studies

501 provide context, degradation in air likely differs due to UV exposure, desiccation, and distinct

502 microbial communities; direct measurements across environmental conditions are a clear

503 priority.

504 **4.4 Minimal tools, maximum reach, and navigating limitations**

505 Perhaps the most striking result from our work is the simplicity and versatility of passive

506 airborne sampling. No pumps or power are needed, and equipment is extremely low cost and

507 easy to deploy. This minimal-infrastructure approach makes it viable for remote headwaters,

508 steep mountain channels, urban stormwater networks, and contaminated waters where sampling

509 is unsafe[48,49]. Despite this being the first study to explore the link between water-to-air eDNA

510 migration, this could open opportunities for future monitoring scenarios where access to water is

511 limited (e.g. droughts, floods and public-health risks such as bacterial outbreaks in stagnant

512 waters) Airborne eDNA may offer resilient pathways for rapid invasive-species alerts, real-time

513   disease surveillance in flood-prone wetlands and non-invasive population censuses in protected

514   spawning grounds.

515   However, air-sampling replication was imbalanced, with two biological replicates for

516   gelatin and PTFE filters and one for MCE filters and the deionized-water tray. This imbalance

517   limits the strength of cross-method contrasts, so future deployments should harmonize

518   replication across sampler types. Our temporal replication comprised six co-located sampling

519   dates during the peak spawning period; while adequate for estimating a system-specific dilution

520   magnitude, this sample size limits inference about temporal drivers and broader applicability.

521   Additionally, our focus on peak spawning, when salmon exhibit maximal surface activity,

522   means that applicability to other seasons, less surface-active species, or lentic systems requires

523   further investigation.

524   Naturally, challenges remain, as passive deployments rely on surface-area-by-time

525   metrics rather than standardized air-volume units, complicating direct comparisons across

526   studies. Optimal exposure times must balance accumulation against DNA degradation from UV,

527   microbes and moisture[45]. Weather variability in wind, humidity and rain can alter deposition

528   rates and sampler efficiency[12,28]. In cold climates, freezing of exposed holders can alter particle

529   deposition and DNA retention, and thaw may physically strip accumulated material;

530   enclosed/rain-shielded housings and shorter deployments could mitigate this, but dedicated cold-

531   weather tests are needed. Further studies should shed light on environmental conditions (i.e.,

532   temperature, humidity, seasons, etc.,) refine sampler design, systematically compare vertical and

533   horizontal orientations, explore automated or drone-based retrieval and integrate river discharge

534   and meteorological data into quantitative models[35,39,50,51]. In particular, upwind/downwind

535   replicate samplers with co-measured wind direction/speed and precipitation would help test

signal provenance. Because we had relatively few time points, the Negative Binomial

overdispersion (φ) parameter was fixed to a literature-supported value and observations from

different gate-opening intervals were treated as independent; with higher-frequency sampling, φ

could be estimated from the data and an explicit temporal autocorrelation term incorporated.

Relatedly, our inference treats per-capita shedding and decay as aggregated into ω and

approximately constant over each 24-h deployment; individual heterogeneity is absorbed into the

residual variance, and future work with size data or mechanistic submodels could relax this

assumption. This study evaluates a single stream/hatchery reach and species; replication across

systems and taxa will be required to assess generality.

Our study begins to chart a portion of airborne eDNA ecology in five key dimensions:[28]
1) we support a local origin by matching airborne DNA trends to co-occurring water eDNA and

fish counts, 2) we highlight likely transport mechanisms such as evaporation, bubble bursts, and

fish activity, 3) we quantify dispersal and dilution across the water-air boundary, 4) we

demonstrate fate through differential deposition on vertical filters and horizontal trays, and

finally, 5) we show that airborne DNA fragments remain amplifiable, offering an initial glimpse

into their molecular state after transport. The potential underlying processes suggest that air

could act as a dilute, but still informative, extension of the aquatic environment, representing

biological signals that are real, quantifiable, and ecologically meaningful. These insights lay the

groundwork for future studies on persistence, degradation and particle-size distributions from

airborne eDNA[52].

567   **Author contributions**

568   Y.C.A.I. conceived the study. Y.C.A.I. G.G and E.A.A. designed the field and laboratory

569   protocols. Y.C.A.I. and G.G. jointly designed the downstream statistical analyses and Bayesian

570   modeling framework. G.G. conducted all statistical analyses, with inputs from R.P.K. The

571   fieldwork was performed by Y.C.A.I. and E.A.A., while Y.C.A.I. and G.G. co-wrote the

572   manuscript. R.P.K. supervised the project, contributed to conceptual guidance, and provided

573   critical revisions. All authors contributed to the study design and approved the final manuscript.

574   **Data availability**

575   The authors declare that they have no competing interests. All data needed to evaluate the

576   conclusions in this paper are available in the main text and/or the Supplementary Materials.

577   Codes are available on https://github.com/gledguri/Air-eDNA-quant. Additional data, code, and

578   materials will be made available upon reasonable request. No materials were subject to material

579   transfer agreements (MTAs).

580

References

582   1. Dudgeon, D. *et al.* Freshwater biodiversity: Importance, threats, status and conservation challenges. *Biological*
583   *Reviews* **81**, 163–182 (2006).

584   2. Reid, A. J. *et al.* Emerging threats and persistent conservation challenges for freshwater biodiversity. *Biological*
585   *Reviews* **94**, 849–873 (2019).

586   3. Biggs, J. *et al.* Using eDNA to develop a national citizen science-based monitoring programme for the great
587   crested newt (*Triturus cristatus*). *Biological Conservation* **183**, 19–28 (2015).

588   4. A. C. Thomas, A. C. *et al.* A system for rapid eDNA detection of aquatic invasive species. *Environmental DNA* **2**,
589   261–270 (2020).

590   5. Wilkinson, S. P. *et al.* TICI: A taxon-independent community index for eDNA-based ecological health
591   assessment. *PeerJ* **12**, e16963 (2024).

592   6. Allan, E. A. *et al.* Quantifying impacts of an environmental intervention using environmental DNA. *Ecological*
593   *Applications* **33**, e2914 (2023).

594   7. Guri, G. *et al.* Predicting trawl catches using environmental DNA. *ICES Journal of Marine Science* **81**, 1536–
595   1548 (2024).

596   8. M. D. Tillotson, M. D. *et al.* Concentrations of environmental DNA (eDNA) reflect spawning salmon abundance
597   at fine spatial and temporal scales. *Biological Conservation* **220**, 1–11 (2018).

598   9. Clare, E. L. *et al.* eDNAir: Proof of concept that animal DNA can be collected from air sampling. *PeerJ* **9**,
599   e11030 (2021).

600   10. Garrett, N. R. *et al.* Airborne eDNA documents a diverse and ecologically complex tropical bat and other
601   mammal community. *Environmental DNA* **5**, 350–362 (2023).

602   11. M. D. Johnson, M. D., Cox, R. D. & Barnes, M. A. Analyzing airborne environmental DNA: A comparison of
603   extraction methods, primer type, and trap type on the ability to detect airborne eDNA from terrestrial plant
604   communities. *Environmental DNA* **1**, 176–185 (2019).

605   12. M. D. Johnson, M. D., Barnes, M. A., Garrett, N. R. & Clare, E. L. Answers blowing in the wind: Detection of
606   birds, mammals, and amphibians with airborne environmental DNA in a natural environment over a yearlong
607   survey. *Environmental DNA* **5**, 375–387 (2023).

608   13. C. Lynggaard, C., Frøslev, T. G., Johnson, M. S., Olsen, M. T. & Bohmann, K. Airborne environmental DNA
609   captures terrestrial vertebrate diversity in nature. *Molecular Ecology Resources* **24**, e13840 (2024).

610   14. Roger, F. *et al.* Airborne environmental DNA metabarcoding for the monitoring of terrestrial insects—A proof
611   of concept from the field. *Environmental DNA* **4**, 790–807 (2022).

612   15. C. Lynggaard,. *et al.* Airborne environmental DNA for terrestrial vertebrate community monitoring. *Current*
613   *Biology* **32**, 701–707.e5 (2022).

614   16. Tournayre, O. *et al.* First national survey of terrestrial biodiversity using airborne eDNA. *Scientific Reports* **15**,
615   19247 (2025).

616   17. Sullivan, A. R. *et al.* Airborne eDNA captures three decades of ecosystem biodiversity. (2023)
617   doi:https://doi.org/10.1101/2023.12.06.569882.

618   18. Klepke, M. J., Sigsgaard, E. E., Jensen, M. R., Olsen, K. & Thomsen, P. F. Accumulation and diversity of
619   airborne, eukaryotic environmental DNA. *Environmental DNA* **4**, 1323–1339 (2022).

620   19. Lynggaard, C. *et al.* Vertebrate environmental DNA from leaf swabs. *Current Biology* **33**, R853–R854 (2023).

621   20. F. Altermatt, M. Couton, L. Carraro, F. Keck, L. Lawson-Handley, F. Leese, X. Zhang, Y. Zhang, R.Blackman,
622   Utilizing aquatic environmental DNA to address global biodiversity targets. *Nature Reviews Biodiversity*, doi:
623   10.1038/s44358-025-00044-x (2025).

624   21. M. Johnson, M. A. Barnes, Macrobial airborne environmental DNA analysis: A review of progress, challenges,
625   and recommendations for an emerging application. *Molecular Ecology Resources* **24**, e13998 (2024).

626   22. C. Folke, S. Polasky, J. Rockström, V. Galaz, F. Westley, M. Lamont, M. Scheffer, H. Österblom, S. R.
627   Carpenter, F. S. Chapin, K. C. Seto, E. U. Weber, B. I. Crona, G. C. Daily, P. Dasgupta, O. Gaffney, L. J. Gordon,
628   H. Hoff, S. A. Levin, J. Lubchenco, W. Steffen, B. H. Walker, Our future in the Anthropocene biosphere. *Ambio* **50**,
629   834–869 (2021).

630   23. Monahan, D. E. C., Spiel, D. E. & Davidson, K. L. A model of marine aerosol generation via whitecaps and
631   wave disruption. in *Oceanic whitecaps* (eds. Monahan, E. C. & Niocaill, G. M.) vol. 2 (Springer, Dordrecht, 1986).

632   24. J. H. Seinfeld, J. H. & Pandis, S. N. *Atmospheric Chemistry and Physics: From Air Pollution to Climate*
633   *Change.* (Wiley, ed. 3, 2016).

634   25. L. Duchemin, L., Popinet, S., Josserand, C. & Zaleski, S. Jet formation in bubbles bursting at a free surface.
635   *Physics of Fluids* **14**, 3000–3008 (2002).

636   26. Mueller, R. P., Southard, S. S., May, C. W., Pearson, W. H. & Cullinan, V. I. Juvenile Coho Salmon Leaping
637   Ability and Behavior in an Experimental Culvert Test Bed. *Transactions of the American Fisheries Society* **137**,
638   941–950 (2008).

639   27. Stell, E., Hoover, J. J., Fuller, L. & Parsons, G. R. Analyzing Leap Characteristics and Water Escape Velocities
640   of Silver Carp Using In Situ Video Analysis. *North American Journal of Fisheries Management* **40**, 163–174
641   (2020).

642   28. A. I. J. M. Van Dijk, L. A. I. J. M., Bruijnzeel, L. A. & Eisma, E. H. A methodology to study rain splash and
643   wash processes under natural rainfall. *Hydrological Processes* **17**, 153–167 (2003).

644   29. W. Chen, J. Wang, Y. Zhao, Y. He, J. Chen, C. Dong, L. Liu, J. Wang, L. Zhou, Contrasting pollution responses
645   of native and non-native fish communities in anthropogenically disturbed estuaries unveiled by eDNA
646   metabarcoding. *Journal of Hazardous Materials* **480**, 136323 (2024).

647   30. D. V. Ruiz-Ramos, R. S. Meyer, D. Toews, M. Stephens, M. K. Kolster, J. P. Sexton, Environmental DNA
648   (eDNA) detects temporal and habitat effects on community composition and endangered species in ephemeral
649   ecosystems: A case study in vernal pools. *Environmental DNA* **5**, 85–101 (2023).

650   31. J. Wan, Z. Zhang, Y. Huo, X. Wang, Y. Wang, J. Wu, M. Huo, Particle Size Matters: Distribution, Source, and
651   Seasonality Characteristics of Airborne and Pathogenic Bacteria in Wastewater Treatment Plants. *Atmosphere* **14**,
652   465 (2023).

653   32. Wu, Y., Shen, F. & Yao, M. Use of gelatin filter and BioSampler in detecting airborne H5N1 nucleotides,
654   bacteria and allergens. *Journal of Aerosol Science* **41**, 869–879 (2010).

655 33. Harnpicharnchai, P. *et al.* AirDNA sampler: An efficient and simple device enabling high-yield, high-quality
656 airborne environment DNA for metagenomic applications. *PLOS ONE* **18**, e0287567 (2023).

657 34. Duda, J. J. *et al.* Environmental DNA is an effective tool to track recolonizing migratory fish following large-
658 scale dam removal. *Environmental DNA* **3**, 121–141 (2021).

659 35. D. W. Welch, & Ishida, Y. On the Statistical Distribution of Salmon in the Sea: Application of the Negative
660 Binomial Distribution, and the Influence of Sampling Effort. *Canadian Journal of Fisheries and Aquatic Sciences*
661 **50**, 1029–1038 (1993).

662 36. Guri, G. *et al.* Quantifying the Detection Sensitivity and Precision of qPCR and ddPCR Mechanisms for eDNA
663 Samples. *Ecology and Evolution* **14**, e70678 (2024).

664 37. A. O. Shelton, A. Ramón-Laca, A. Wells, J. Clemons, D. Chu, B. E. Feist, R. P. Kelly, S. L. Parker-Stetter, R.
665 Thomas, K. M. Nichols, L. Park, Environmental DNA provides quantitative estimates of Pacific hake abundance
666 and distribution in the open ocean. *Proceedings of the Royal Society B: Biological Sciences* **289**, 20212613 (2022).

667 38. Wood, Z. T. *et al.* Spatial Heterogeneity of eDNA Transport Improves Stream Assessment of Threatened
668 Salmon Presence, Abundance, and Location. *Frontiers in Ecology and Evolution* **9**, 650717 (2021).

669 39. K. A. Prather, T. H. Bertram, V. H. Grassian, G. B. Deane, M. D. Stokes, P. J. DeMott, L. I. Aluwihare, B. P.
670 Palenik, F. Azam, J. H. Seinfeld, R. C. Moffet, M. J. Molina, C. D. Cappa, F. M. Geiger, G. C. Roberts, L. M.
671 Russell, A. P. Ault, J. Baltrusaitis, D. B. Collins, C. E. Corrigan, L. A. Cuadra-Rodriguez, C. J. Ebben, S. D.
672 Forestieri, T. L. Guasco, S. P. Hersey, M. J. Kim, W. F. Lambert, R. L. Modini, W. Mui, B. E. Pedler, M. J. Ruppel,
673 O. S. Ryder, N. G. Schoepp, R. C. Sullivan, D. Zhao, Bringing the ocean into the laboratory to probe the chemical
674 complexity of sea spray aerosol. *Proceedings of the National Academy of Sciences* **110**, 7550–7555 (2013).

675 40. Abrego, N. *et al.* Airborne DNA reveals predictable spatial and seasonal dynamics of fungi. *Nature* **631**, 835–
676 842 (2024).

677 41. Giolai, M. *et al.* Measuring air metagenomic diversity in an agricultural ecosystem. *Current Biology* **34**, 3778–
678 3791.e4 (2024).

679 42. Galbán, S., Justel, A., González, S. & Quesada, A. Local meteorological conditions, shape and desiccation
680 influence dispersal capabilities for airborne microorganisms. *Science of The Total Environment* **780**, 146653 (2021).

681 43. Maki, T. *et al.* Vertical distribution of airborne microorganisms over forest environments: A potential source of
682 ice-nucleating bioaerosols. *Atmospheric Environment* **302**, 119726 (2023).

683 44. Jager, H., Trimbos, K. B., Luursema, J.-M., Speksnijder, K. A. G. C. L. & Stewart, K. A. A breath of fresh air:
684 Comparative evaluation of passive versus active airborne eDNA sampling strategies. (2025)
685 doi:10.1101/2025.03.26.645491). https://doi.org/10.1101/2025.03.26.645491.

686 45. Blanchard, D. C. & Woodcock, A. H. The production, The production, concentration, and vertical distribution of
687 the sea-salt aerosol. *Annals of the New York Academy of Sciences* **338**, 330–347 (1980).

688 46. Hinds, W. C. & Zhu, Y. *Aerosol Technology: Properties, Behavior, and Measurement of Airborne Particles*.
689 (John Wiley & Sons, 2022).

690 47..Herman, B. A. Use of foreign eDNA tracers to resolve site- and time-specific eDNA distributions in natural
691 streams. (Humboldt State University, 2023).

692 48. Brandão-Dias, P. F. P. *et al.* Particle size influences decay rates of environmental DNA in aquatic systems.
693 *Molecular Ecology Resources* **23**, 756–770 (2023).

694 49. K. M. Strickler, A. K. M., Fremier, A. K. & Goldberg, C. S. Quantifying effects of UV-B, temperature, and pH
695 on eDNA degradation in aquatic microcosms. *Biological Conservation* **183**, 85–92 (2015).

696 50. Barnes, M. A. & Turner, C. R. The ecology of environmental DNA and implications for conservation genetics.
697 *Conservation Genetics* **17**, 1–17 (2016).

698 51. Harrison, J. B., Sunday, J. M. & Rogers, S. M. Predicting the fate of eDNA in the environment and implications
699 for studying biodiversity. *Proceedings of the Royal Society B: Biological Sciences* **286**, 20191409 (2019).

700 52. Bagley, M. *et al.* High-throughput environmental DNA analysis informs a biological assessment of an urban
701 stream. *Ecological Indicators* **104**, 378–389 (2019).

702 53. Kirchgeorg, S. *et al.* eProbe: lSampling of Environmental DNA within Tree Canopies with Drones.
703 *Environmental Science & Technology* **58**, 16410–16420 (2024).

704 54. Shogren, A. J. *et al.* Controls on eDNA movement in streams: Transport, Retention, and Resuspension. *Scientific
705 Reports* **7**, 5065 (2017).

706 55. Brandão-Dias, P. F. *et al.* Differential decay of multiple environmental nucleic acid components. *Scientific
707 Reports* **15**, 26791 (2025).